Journal of Power Sources 224 (2013) 115–119

Contents lists available at SciVerse ScienceDirect

Journal of Power Sources

journal homepage: www.elsevier.com/locate/jpowsour

Short communication

Catalyst-free porous carbon cathode and ionic liquid for high efficiency, rechargeable Li/O_2 battery

Francesca Soavi, Simone Monaco, Marina Mastragostino*

Dipartimento di Scienza dei Metalli, Elettrochimica e Tecniche Chimiche, University of Bologna, Via San Donato15, 40127 Bologna, Italy

HIGHLIGHTS

- Catalyst-free porous carbon and ionic liquid are investigated for Li/O_2 batteries.
- Low recharge potential and good cycling efficiency of carbon cathode are reported.
- Meso-macroporous carbon is obtained by a simple, low-cost template synthesis.

ARTICLE INFO

Article history:
Received 31 July 2012
Received in revised form
7 September 2012
Accepted 27 September 2012
Available online 4 October 2012

Keywords:
Lithium/O_2 battery
Ionic liquid
Oxygen redox reaction
Porous carbon

ABSTRACT

Li/O_2 batteries are a breakthrough in battery technology for powering long-range electric vehicles. The viability of high efficiency, rechargeable Li/O_2 battery is demonstrated by the use of catalyst-free meso-macroporous carbon cathode and N-butyl-N-methyl pyrrolidinium bis(trifluoromethanesulfonyl)imide ionic liquid-based electrolyte. The carbon electrode, obtained by a simple, low-cost template method, features a high specific capacity of 2500 mAh g^{-1} at 2.6 V vs. Li^+/Li and, more importantly, a recharge potential lower than 3.8 V vs Li^+/Li that prevents secondary reactions in the ionic liquid detrimental for battery rechargeability and makes it possible to reach a recharge efficiency of 90%.

1. Introduction

Given their extremely high theoretical energy, Li/O_2 batteries are at cutting-edge research of electrochemical energy storage systems for powering long-range electric vehicles. The core of these batteries is the oxygen redox reaction (ORR) at the cathode that governs capacity and rechargeability [1–4]. In non-aqueous, secondary Li/O_2 batteries, the expected cell reactions are:

$$2Li + O_2 \leftrightarrows Li_2O_2 \quad (1)$$

and

$$2Li + \tfrac{1}{2}O_2 \leftrightarrows Li_2O \quad (2)$$

Li_2O and Li_2O_2 are insoluble species that progressively insulate the electrode upon discharge, thus affecting cathode discharge capacity and causing high overpotentials during battery recharge [1–4]. Chemical and electrochemical electrolyte stability is of paramount importance in order to make secondary Li/O_2 batteries work with reactions (1) and/or (2). It has been reported that conventional solvents, particularly carbonate-based ones, irreversibly decompose upon cell discharge and oxidize at the potentials required for cell recharge; such processes are even favored by the high reactivity of superoxide [5–7]. Recently, cell rechargeability has been investigated by the use of electrolytes with tetraethylene glycol dimethyl ether (TEGDME) or dimethylsulfoxide with catalyzed electrodes [8,9].

The need of high chemically and electrochemically stable and low volatile solvents thus makes ionic liquids (ILs) very attractive media for Li/O_2 batteries. The IL class includes a variety of room temperature molten salts, and the pyrrolidinium-based ones feature a favorable combination of such physicochemical properties as low vapor pressure, low flammability, high thermal stability, good ionic conductivity, wide electrochemical stability window and hydrophobicity [10,11]. Exceptionally high stability of superoxide has been demonstrated in pyrrolidinium salts of bis(trifluoromethanesulfonyl)imide (TFSI), which in turn means low reactivity of the radical anion towards such

* Corresponding author. Tel.: +39 (0)512099798; fax: +39 (0)512099365.
E-mail address: marina.mastragostino@unibo.it (M. Mastragostino).

0378-7753/$ – see front matter © 2012 Elsevier B.V. All rights reserved.
http://dx.doi.org/10.1016/j.jpowsour.2012.09.095

ILs [12]. ORR has recently been investigated in IL-lithium salt solutions, but so far only very few papers report the cyclability of Li/O_2 batteries operating with such media [13–16]. Even a mixture of $PYR_{14}TFSI$:TEGDME-$LiCF_3SO_3$ (1:1) has been investigated [17].

The specific capacity of Li/O_2 batteries is notably affected by cathode composition and porosity. While ORR is promoted by catalysts that are typically supported or mixed with high surface area carbons, the role played in ORR by catalysts is still unclear [1–3]. Furthermore, a high specific meso-macroporous volume of the carbon favors cathode capacity because it makes it possible to host high amounts of Li_2O_2 (s) and Li_2O (s) discharge reaction products. The discharge capacity of cathodes operating in conventional organic electrolyte is mainly related to carbon specific pore volume and pore size and is not much affected by carbon specific-surface area. Then, too, carbon surface chemistry, including carbon doping with heteroatoms like nitrogen or boron, has been demonstrated to be crucial for ORR [3,18–23].

Here we report the use of catalyst-free meso-macroporous carbon (ZL) electrodes as high efficiency cathodes for Li/O_2 battery operating with N-butyl-N-methyl pyrrolidinium bis(trifluoromethanesulfonyl) imide ($PYR_{14}TFSI$) IL.

2. Experimental

ZL meso-macroporous carbon was prepared using a formaldehyde (*F*, >37% Fluka)-resorcinol (R, puriss. p.a. Riedel-de-Haën) resin as a carbon precursor and commercial colloidal silica (40% SiO_2, 70–100 nm, SNOWTEX ZL, NISSAN CHEMICAL INDUSTRIES, Ltd.) as template [24]. Resorcinol was first completely dissolved in the aqueous formaldehyde solution and then silica added with 1:2:2 R:F:SiO_2 molar ratio. The mixture was aged at 80–90 °C for few days, followed by carbonization with a ramp of 10 °C min^{-1} at 900 °C for 2 h, under Ar flow (200 cc min^{-1}) by an ELITE furnace. The pyrolyzed powder was milled and silica template was then removed by 6 M NaOH hydroalcoholic solution. The carbon was carefully rinsed with H_2O/ethanol and dried at 60 °C over night. The residual SiO_2, checked by thermogravimetry under O_2 flow, was 2%. The porosity of the template carbon was evaluated by Brunauer, Emmett and Teller (B.E.T.) and Density Functional Theory (DFT) analyses of the N_2 adsorption isotherm at 77 K, which was collected with an ASAP 2020 system (Micromeritics); the carbon was dried for at least 2 h at 120 °C before testing.

ORR on ZL carbon was investigated by cyclic voltammetry (CV) and galvanostatic measurements at carbon coated glassy carbon (GC, Tokai Carbon Ltd., 0.28 cm^2 coating area) or carbon paper (CP, Spectracarb 2050, Spectracorp, 0.35 cm^2 coating area) electrodes in a 5 mL cell that was thermostated at 30 °C and 60 °C by a HAAKE K40 thermocryostat. Electrodes were coated by evaporation at 60 °C for several hours of aliquots of carbon (28 mg mL^{-1}) – polyvinylidene fluoride (PVDF, KYNAR HSV900, 1.4 mg mL^{-1}) – N-methyl pyrrolidone (NMP, Fluka, >99.0%) ink that was sonicated before use. CV tests were also performed at bare GC electrode (GC, Tokai Carbon Ltd., 0.071 cm^2 electrode area) for comparison.

The reference electrode was a silver wire in 6.10^{-2} M AgTFSI (97%, Aldrich) – $PYR_{14}TFSI$ (3.6 V vs Li^+/Li). A Pt counter electrode was used for the CVs and a lithium foil for the galvanostatic measurements. The electrolyte was $PYR_{14}TFSI$ (99.5%, Solvionic)–0.1 M LiTFSI (3 M); $PYR_{14}TFSI$ was dried overnight at 80 °C (Büchi Glass Oven B-580) before use, LiTFSI was stored in dry box (MBraun, O_2 and H_2O < 1 ppm) and used as received. Oxygen (>99.999%, SIAD) was bubbled through the cell for at least 30 min before the CVs and was continuously flowed for the galvanostatic discharge and interrupted under charge. The electrochemical tests were performed with a PerkinElmer VSP multichannel potentiostat/galvanostat. The voltammetric scans were corrected for the ohmic drop evaluated by impedance spectroscopy in the 10 kHz–1 Hz range.

Scanning electron microscopy observations (SEM) and energy dispersion spectroscopy (EDS) were carried out with a ZEISS EVO 50 apparatus equipped with an energy dispersive X-ray analyzer from Oxford model INCA ENERGY350 system.

X-ray diffraction measurements (XRD) were performed with a Philips X'Pert diffractometer, a Cu Kα (λ = 1.5406 Å) radiation source and Ni filter by continuous (0.05° 2θ s^{-1} scan rate) or step scanning (0.005° 2θ s^{-1} scan rate) mode; crystallite size was evaluated by the Sherrer's analysis of the main diffraction peak. For XRD analyses, cycled electrodes were carefully protected from air by a thin Mylar film. The Raman spectra were recorded by a Raman Microscope RENISHAW Mod. INVIA with Argon ion laser (λ = 514 nm, 4 scans, 10 s per scan, 1.4 cm^{-1} resolution).

3. Results and discussion

The ZL carbon was obtained by a simple, low-cost template method and tested by porosity and structural and electrochemical analyses. Fig. 1a shows the incremental pore volume of the carbon featuring a meso-macroporous texture with pore size distribution centered at 54 nm and a specific volume from pores with diameters between 2 nm and 100 nm of 0.73 cm^3 g^{-1} (Table S1). Porosity in the macropore domain is evinced by the SEM image reported in Fig. 1b. XRD (Fig. S1) and Raman (Fig. S2) analyses indicate that ZL is an amorphous carbon made of small graphitic domains of ca. 2 graphene layers 2.5 nm wide. The I_{D1}/I_G height ratio of the Raman bands D1 attributed to graphene layer edges and G, corresponding to the in-plane vibrational mode of surface graphene layers, is 1.7.

Fig. 2a shows the voltammetric response of bare (GC) and ZL-coated (ZL/GC) glassy carbon electrodes in O_2-saturated $PYR_{14}TFSI$–0.1 M LiTFSI, at 20 mV s^{-1} and 30 °C. The voltammetric reduction peak at the bare GC at 2.05 V vs. Li^+/Li is related to the oxygen reduction to superoxide that because of the presence of lithium ions further reacts to give insoluble products on the electrode surface. These products are, then, oxidized in the back anodic scan featuring a narrow peak at 3.17 V vs. Li^+/Li and a broader one in the 3.5–4.3 V vs. Li^+/Li region [13–15]. Similar features were also observed by performing ORR studies in conventional organic electrolyte; on the basis of *in situ* spectroscopy measurements the former anodic peak was attributed to lithium superoxide oxidation and the latter to the oxidation of lithium peroxide which is generated by LiO_2 disproportion [25]. In Fig. 2a, the oxygen reduction charge at GC is 3.9 mC cm^{-2}, and the efficiency of the recharge process, calculated on the entire anodic scan, is 92%, a high value that is achievable thanks to the wide electrochemical stability window of the IL. The CV at the ZL/GC electrode, free from any additional catalyst, features an oxygen reduction peak that is

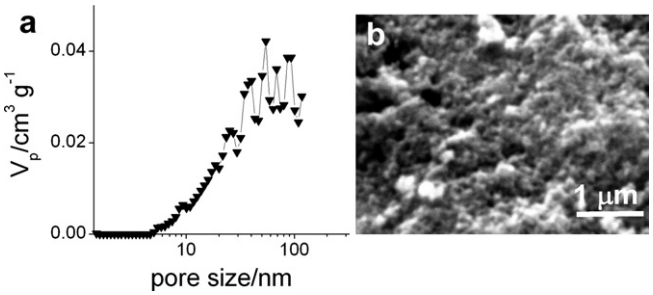

Fig. 1. (a) Incremental pore volume distribution (V_p) and (b) SEM image of the ZL carbon.

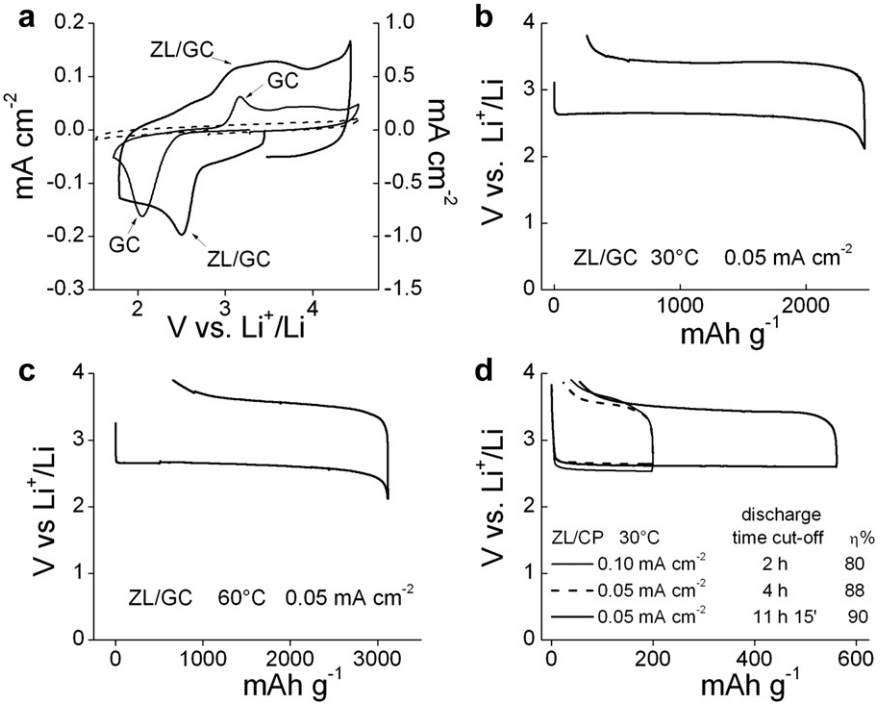

Fig. 2. (a) CVs at 20 mV s^{-1} and 30 °C of bare (GC, left *y*-axis) and ZL-coated (ZL/GC, 0.5 mg cm^{-2} of ZL, right *y*-axis) glassy carbon electrodes in O_2-saturated $PYR_{14}TFSI$–0.1 M LiTFSI (dashed line is the CV of GC before O_2 saturation); voltage profiles upon galvanostatic discharge/charge of the ZL/GC electrode (0.5 mg cm^{-2} of ZL carbon) at 0.05 mA cm^{-2} and (b) 30 °C and (c) 60 °C and (d) of the ZL/CP electrode (1.0 mg cm^{-2} of ZL carbon) at 0.1 and 0.05 mA cm^{-2} at 30 °C in O_2-saturated $PYR_{14}TFSI$–0.1 M LiTFSI.

anticipated by ca. 500 mV. The cathodic peak is shifted to 2.5 V vs. Li^+/Li and this can be related to the porous carbon nanotexture: ZL is a low graphitic carbon with a high number of exposed graphene edges that favor O_2-adsorption and reduction. Furthermore, a large 3.0–3.9 V vs. Li^+/Li reoxidation region appears which corresponds to the overlapping of the two anodic peaks observed at the GC electrode. The high surface area of the ZL carbon accounts for voltammetric current densities that are much higher than those observed with the bare GC and causes a large background current that overlaps the faradic ORR process (the background current linearly increases with the scan rate, as expected for a double-layer capacitive carbon electrode). The oxygen reduction charge at this electrode is 45 mC cm^{-2} with a recharge efficiency of 97%. These results indicate that the nature of the ZL carbon electrode notably influences ORR and should be beneficial for the capacity and the discharge/charge potentials of the Li/O_2 battery cathode.

This is further demonstrated by the galvanostatic studies. Fig. 2b reports the voltage profile of the catalyst-free ZL/GC electrode upon galvanostatic discharge/charge at 0.05 mA cm^{-2} and 30 °C with 2.0 and 3.8 V vs. Li^+/Li voltage cut-offs. The sharp variation of the voltage profiles clearly indicates the end of the oxygen electrode discharge and recharge processes. Upon discharge, the active area of the ZL/GC electrode is progressively clogged by insoluble oxygen reduction species and at the end of discharge the overvoltage abruptly increases. The recharge ends when the insoluble species are reoxidized and the electrode active area is recovered.

In agreement with the voltammetric results, the electrode discharge takes place at 2.65 V vs. Li^+/Li. The recharge is at 3.4 V vs. Li^+/Li, well below the anodic stability limit of the IL-based electrolyte (4.5 V vs. Li^+/Li, at ZL electrode). The flat charge plateau indicates that only one species is involved, presumably Li_2O_2. Indeed, superoxide oxidation is not detectable because the discharge reported in Fig. 2b lasts ca. 24 h, and hence any produced LiO_2 has time to completely disproportionate to Li_2O_2 [25]. The recharge takes place at potentials that are lower than those reported in literature thus far for Li/O_2 cathodes working with organic or IL-based electrolytes [2–4,16,17]. The low charge voltage makes it possible to achieve a recharge efficiency (η) of 90%, which to our knowledge is the highest value reported up to now for discharge/charge cycles not limited by time; the charge was stopped when the electrode potential abruptly increased. No charge plateau was observed when the ZL/GC electrode was polarized up to 3.8 V vs. Li^+/Li without being previously discharged (Fig. S3).

The discharge capacity of the ZL/GC electrode is of ca. 2500 mAh g^{-1} at the lowest current density and decreases to ca. 1500 mAh g^{-1} when current density doubles. The O_2 flow in the cell is of crucial importance. Indeed, interruption of O_2 bubbling abruptly lowers the electrode discharge potential, which is then restored when O_2 flow is re-established. Fig. 2c reports the voltage profile of the ZL/GC electrode upon the galvanostatic discharge/charge at 0.05 mA cm^{-2} and 60 °C and demonstrates the viability of the $PYR_{14}TFSI$-based electrolyte in Li/O_2 batteries operating above room temperature, where the use of conventional solvents is critical. The electrode capacity is 25% higher at 60 °C than at 30 °C, presumably because of the higher solubility of Li_2O_2 at the higher temperature, and η is ca 80% at 60 °C.

Fig. 2d gives the voltage profiles of ZL-coated carbon paper electrodes (ZL/CP) during cycles that were performed at different discharge time cut-offs, at 30 °C and different current densities. The amount of charge involved in electrode charging is related to that of the discharge step, with a recharge efficiency as high as 90% for the longest discharge. The fact that the longer the discharge time, the higher is the reoxidation charge suggests that parasitic reactions upon discharge are not very important. Furthermore, the increase of efficiency with depth of discharge can be explained by taking into account that the increase of discharge time should increase peroxide anion concentration and, hence, Li_2O_2 solubility should lower. Consequently, more Li_2O_2 is formed on the electrode and

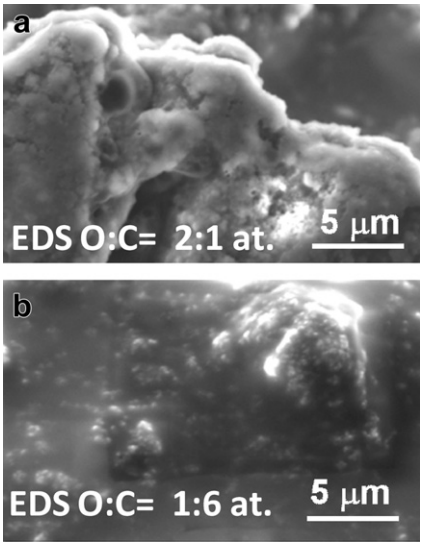

Fig. 3. SEM images of the ZL/CP electrodes (1.0 mg cm^{-2} of ZL carbon) cycled at 0.1 A g^{-1} after 20 h-discharge (a) and after the first recharge (b); the EDS O:C atomic ratio is also reported.

can be reoxidized in the following charge. The increase of current density from 0.05 to 0.10 mA cm^{-2} only slightly affects discharge and charge voltage plateaux, which respectively lower from 2.6 V to 2.5 V vs. Li$^+$/Li and increase from 3.55 V up to 3.65 V vs. Li$^+$/Li.

In order to unambiguously ascribe the charge plateau to the reoxidation of oxygen-reduced species formed during discharge, the ZL/CP electrodes were analyzed by SEM-EDS, XRD and Raman spectroscopy. The SEM-EDS analysis reported in Fig. 3 indicates the formation of oxygen-rich products upon electrode discharge; the O to C atomic ratio changed from 2:1 in the discharged electrode to 1:6 in the charged one.

XRD and Raman spectroscopy patterns in Fig. 4 unambiguously identified such oxygen-based species as Li_2O_2; no secondary ORR products were detected.

XRD analysis of the discharged electrode indicates that Li_2O_2 crystallites are 42 nm wide, a size that well fits the ZL carbon pore size. If we take into account that the Li_2O_2 density is 2.3 g cm^{-3} and the meso-macropore volume of ZL is 0.73 cm^3 g^{-1}, then 1.7 g of peroxide per gram of carbon are required to clog ZL pores, which

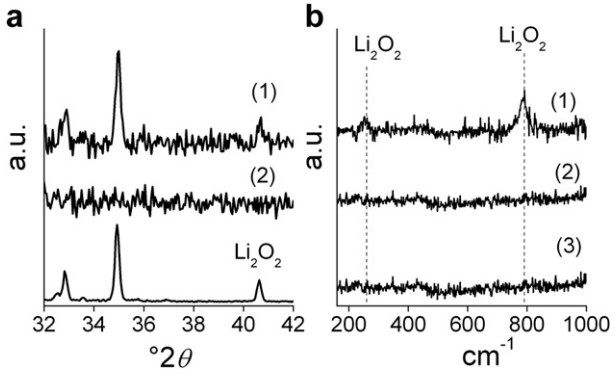

Fig. 4. (a) XRD of ZL/CP electrodes (1.0 mg cm^{-2} of ZL carbon) cycled at 0.1 A g^{-1} after 20 h-discharge (1) and after the first recharge (2), the pattern of the Li_2O_2 powder is also reported; (b) Raman spectra of the fully discharged (1) and charged (2) ZL/CP electrodes and of the ZL carbon powder (3).

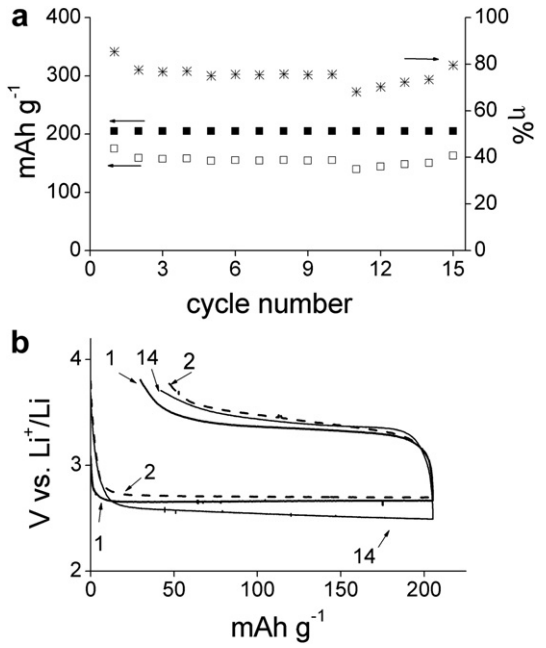

Fig. 5. (a) Discharge (■) and charge (□) specific capacities and recharge efficiency (✳) and (b) potential profiles over cycling of a ZL/GC electrode (ca. 2 mg cm^{-2} of ZL) at 0.08 mA cm^{-2} with discharge time cut-off of 5 h and charge potential cut-off of 3.8 V vs. Li$^+$/Li up to the 10th cycle and 3.7 V vs. Li$^+$/Li for the following cycles (labels indicate cycle numbers).

corresponds to a charge of ca. 2000 mAh g^{-1}, which compares well to the specific capacity data of ZL reported above.

Fig. 5 reports the trend of the specific discharge and charge capacities and recharge efficiency and of the electrode potential profiles over repeated cycles of a ZL/GC electrode at ca. 0.08 mA cm^{-2} with discharge time cut-off of 5 h, corresponding to ca. 0.4 mAh cm^{-2} and 200 mAh g^{-1}. The recharge was not time limited and, as shown in Fig. 5b, it took place below 3.8 V vs. Li$^+$/Li in all cycles. The recharge efficiency was ca. 80% because of the low depth of discharge. FTIR spectroscopy was used to test the electrolyte solution before and after cycling and did not reveal any IL-decomposition products; Fig. 6 shows only minor changes in the spectra due to conformational effects and related to the variation of Li$^+$ concentration [26]. These data indicate a good cycling stability of the ZL carbon in PYR$_{14}$TFSI-based electrolyte. However, the lithium anode side has to be investigated in order to fully assess a long cycle life of a Li/O_2 cell with these cathode and electrolyte.

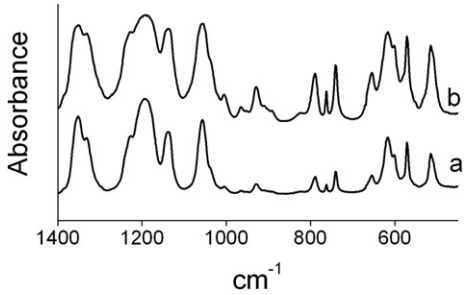

Fig. 6. FITR spectra of the PYR$_{14}$TFSI–0.1 M LiTFSI solution (a) fresh and (b) after 1 week's cycling.

4. Conclusions

Meso-macroporous carbon obtained by a simple, low-cost template synthesis and commercial $PYR_{14}TFSI$-based IL provide a real possibility for the development of rechargeable Li/O_2 batteries that can safely operate even above room temperature.

Acknowledgments

Work funded by the European Commission in the Seventh Framework Programme FP7-2010-GC-ELECTROCHEMICAL STORAGE, under contract no. 265971 "Lithium-Air Batteries with split Oxygen Harvesting and Redox processes" (LABOHR). All the partners of the LABOHR Project are acknowledged for the fruitful discussions on Li/O_2 batteries with ionic liquids.

Appendix A. Supplementary data

Supplementary data related to this article can be found at http://dx.doi.org/10.1016/j.jpowsour.2012.09.095.

References

[1] A. Kraytsberg, Y. Ein-Eli, J. Power Sources 196 (2011) 886–893.
[2] J. Christensen, P. Albertus, R.S. Sanchez-Carrera, T. Lohmann, B. Kozinsky, R. Liedtke, J. Ahmed, A. Kojic, J. Electrochem. Soc. 159 (2012) R1–R30.
[3] R. Padbury, X. Zhang, J. Power Sources 196 (2011) 4436–4444.
[4] P.G. Bruce, S. Freunberger, L.J. Hardwick, J.-M. Tarascon, Nat. Mater. 11 (2012) 19–29.
[5] S.A. Freunberger, Y. Chen, Z. Peng, J.M. Griffin, L.J. Hardwick, F. Bardé, P. Novák, P.G. Bruce, J. Am. Chem. Soc. 133 (2011) 8040–8047.
[6] B.D. McCloskey, D.S. Bethune, R.M. Shelby, G. Girishkumar, A.C. Luntz, J. Phys. Chem. Lett. 2 (2011) 1161–1166.
[7] R. Black, S.H. Oh, J. Lee, T. Yim, B. Adams, L.F. Nazar, J. Am. Chem. Soc. 134 (2012) 2902–2905.
[8] C.Ó. Laoire, S. Mukerjee, E.J. Plichta, M.A. Hendrickson, K.M. Abraham, J. Electrochem. Soc. 158 (2011) A302–A308.
[9] Z. Peng, S.A. Freunberger, Y. Chen, P.G. Bruce, Science 337 (2012) 563–566.
[10] A. Lewandoski, A. Swiderska-Mocek, J. Power Sources 194 (2009) 601–609.
[11] G.B. Appetecchi, M. Montanino, M. Carewska, M. Moreno, F. Alessandrini, S. Passerini, Electrochim. Acta 56 (2011) 1300–1307.
[12] M. Hayyan, F.S. Mjalli, M. Ali Hashim, I.M. AlNashef, S.M. Al-Zahrani, K. Lam Chooi, J. Electroanal. Chem. 664 (2012) 26–32.
[13] F. De Giorgio, F. Soavi, M. Mastragostino, Electrochem. Commun. 13 (2011) 1090–1093.
[14] C.J. Allen, S. Mukerjee, E.J. Plichta, M.A. Hendrickson, K.M. Abaham, J. Phys. Chem. Lett. 2 (2011) 2420–2424.
[15] S. Monaco, A.M. Arangio, F. Soavi, M. Mastragostino, E. Paillard, S. Passerini, Electrochim. Acta 83 (2012) 94–104.
[16] A. Garsuch, D.M. Badine, K. Leitner, L.H.S. Gasparotto, N. Borisenko, F. Endres, M. Vracar, J. Janek, R. Oesten, Z. Phys. Chem. 226 (2012) 107–119.
[17] L. Cecchetto, M. Salomon, B. Scrosati, F. Croce, J. Power Sources 213 (2012) 233–238.
[18] X. Yang, P. He, Y. Xia, Electrochem. Commun. 11 (2009) 1127–1130.
[19] J. Xiao, D. Wang, W. Xu, D. Wang, R.E. Williford, J. Liu, J. Zhang, J. Electrochem. Soc. 157 (2010) A487–A492.
[20] G.O. Shitta-Bey, M. Mirzaeian, P.J. Hall, J. Electrochem. Soc. 159 (2012) A315–A320.
[21] C. Tran, J. Kafle, X. Yang, D. Qu, Carbon 49 (2011) 1266–1271.
[22] Y. Li, J. Wang, X. Li, J. Liu, D. Geng, J. Yang, R. Li, X. Sun, Electrochem. Commun. 13 (2011) 668–672.
[23] L. Yang, S. Jiang, Y. Zhao, L. Zhu, S. Chen, X. Wang, Q. Wu, J. Ma, Y. Ma, Z. Hu, Angew. Chem. Int. Ed. 50 (2011) 7132–7135.
[24] S. Han, K.T. Lee, S.M. Oh, T. Hyeon, Carbon 41 (2003) 1049–1056.
[25] Z. Peng, S.A. Freunberger, L.J. Hardwick, Y. Chen, V. Giordani, F. Bardé, P. Novák, D. Graham, J.M. Tarascon, P.G. Bruce, Angew. Chem. Int. Ed. 50 (2011) 6351–6355.
[26] M. Herstedt, M. Smirnov, P. Johansson, M. Chami, J. Grondin, L. Servant, J.C. Lassègues, J. Raman Spectrosc. 36 (2005) 762–770.